ELSEVIER

Electroencephalography and clinical Neurophysiology 98 (1996) 478–483

The equivalent source technique and cortical imaging

Yao Dezhong

Department of Automation, University of Electronic Science and Technology of China, Chengdu City, 610054, China

Accepted for publication: 25 January 1996

Abstract

As an equivalent source localisation technique, the radial dipole source has been chosen as the equivalent source of the actual neural source in the recently developed cortical imaging technique (CIT). In this short paper, the point current source is numerically tested as a new kind of equivalent source for implementing CIT. The results confirm the efficiency of the new equivalent source.

Keywords: Cortical imaging; Equivalent dipole source; Equivalent point current source

1. Introduction

In recent years, a method for simulating the electric potentials on the surface of the brain has been introduced (Sidman et al., 1990; Sidman, 1991; Kearfott et al., 1991). This method consists of the construction of a layer of radially oriented current dipoles in a conducting sphere that simulates the head so that the voltages generated by the layer would take the values measured on the surface of the medium (the scalp). The harmonic potential function for this layer is then evaluated in the interior of the medium in an attempt to approximate the potentials that would be generated by the actual neural sources but which could not be observed without recourse to invasive recording techniques (Sidman et al., 1992). Numerical and experimental tests have been completed for this technique (CIT), and the results are very encouraging (Kearfott et al., 1991; Sidman et al., 1991, 1992; Ford et al., 1993; Wang et al., 1993).

Physically, CIT is an equivalent source technique (Dampney, 1969), the potential produced by the constructed radial dipole layer is assumed to be approximately equivalent to the actual potential produced by the actual neural source (Sidman et al., 1990; Kearfott et al., 1991). In this short paper, a new kind of equivalent source, the point current source, is numerically tested and compared with the current dipole source in implementing CIT ,and the results confirm the efficiency of the point current as an alternative equivalent source in cortical imaging.

2. Outline of the equivalent source cortical imaging technique

Here we outline the CIT developed by Sidman et al. using the equivalent source technique. Let the head be simulated by a homogeneous sphere of radius 1.0 as in Fig. 1. Also suppose that N equivalent sources of unit strength are placed on a spherical shell, the 'test' surface, of radius r_T. This test surface is within and concentric to the surface of the head. A typical equivalent source D_i is located at Cartesian coordinates x_i, = $r_T \cos\theta_i \sin\psi_i$, y_i = $r_T \sin\theta_i \sin\psi_i$, $z_i = r_T \cos\psi_i$,with respect to the coordinate axes.

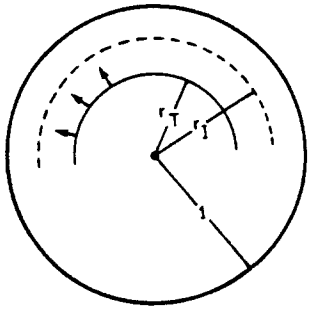

Fig. 1. The 'head' is simulated by a sphere of radius 1.0. Test equivalent sources of unit strength are distributed on a hemispheric shell of radius r_T. Contur plots of the potential generated by the test layer are constructed on a hemispheric shell radius r_I.

PII S0921-884X(96)94694-2

EEG 94694

The potential generated by any such equivalent source can be calculated in the closed form $V(D_i,P_i)$ given in Appendix A, where P_i lies within or on the unit sphere simulating the head. If $V_1,\ldots,V_M$ are voltages measured at scalp recording sites $A_1,\ldots A_M$, it is certainly possible to calculate weighting numbers $u_1,\ldots,u_N$ to satisfy the M equations

$$\sum_{i=1}^{N} u_i V(D_i, A_j) = V_j, \quad \text{for } j = 1,\ldots,M \tag{1}$$

Generally, $M < N$, so that Eq. (1) is an under-determined system of equations with an infinite number of solutions. However, there is a unique solution that minimises $(u_1^2 + \cdots + u_N^2)^{1/2}$, which is the L_2 norm of $(u_1,\ldots,u_N)$. The singular value decomposition (SVD) is used to compute the unique solution of Eq. (1) of minimum norm. In this work, all the singular values are remaindered for no noise existence in the artificial data except for rounding-off error.

In the following numerical tests, the equivalent sources of unit strength were placed on the surface of the spherical shell with radius r_T, at positions whose angles in the standard spherical coordinate system were θ_k and ψ_m, where $\theta_k = (k-1)(2\pi/10)$, $1 \le k \le 10$ and $\psi_m = m(\pi/2)/16$, $1 \le m \le 16$. Hence $N = 160$. The number of scalp electrode sites in the following tests was 33, and they were distributed uniformly on the surface of the upper hemisphere (in order to avoid any effect of prior information about the actual sources on the imaging quality, the uniform distribution is the best choice as noted in Wang et al. (1993)).

Once the values $u_1,\ldots,u_N$ have been calculated one can use the principle of superposition and formulae in Appendix A to compute an approximate image of the potential field on any intermediate spherical shell of radius r_I. Note that $r_T < r_I \le 1.0$. This image surface can include a shell simulating the surface of the brain. As the formulae can be used to calculate theoretical potentials at any point of the shell $r = r_I$, the subsequent scalp topographical maps are constructed by interpolating 160 potential values on the grid on $r = r_I$ corresponding to the grid on $r = r_T$ on which the test equivalent sources $D_1,\ldots,D_{160}$ are placed.

In the present CIT (Sidman et al., 1990), only the radial dipole was used as the equivalent source (referred to as DCIT below), in the following tests, the point current (referred to as CCIT below) is tested as a new kind of equivalent source for implementing cortical imaging.

3. Numerical tests

3.1. Test 1: imaging pair of dipoles

Let us assume that a pair of dipole sources are located at Cartesian coordinates $(x,y,z) = (\pm 0.3 \sin(\pi/6), 0.0, 0.3\cos(\pi/6))$ and that their dipole moments are $(p_x,p_y,p_z) = (\pm 0.5 \sin(\pi/6), 0.0, 0.5\cos(\pi/6))$. The maximum relative imaging errors of the CCIT and DCIT, shown in Table 1, suggest that the best r_T for CCIT may be between 0.35 and 0.45, and that for DCIT r_T had better be smaller than 0.45 for the case tested here although 0.45 has been chosen empirically as the most effective depth to place the test dipoles in previous publications (Kearfott et al., 1991; Wang et al., 1993). Besides, the imaging error of the DCIT increases more quickly than CCIT when the difference of r_I and r_T tends to zero. Fig. 2 shows a few imaging maps of the CCIT and DCIT for $r_T = 0.35$, they demonstrate that both CCIT and DCIT may produce acceptable imaging results for a pair of actual dipoles if the r_T is chosen properly.

Table 1
The maximum relative imaging errors

r_I	r_T					
	0.55		0.45		0.35	
	(1)	(2)	(1)	(2)	(1)	(2)
1.0	5.84×10^{-3}	6.21×10^{-3}	3.43×10^{-3}	3.04×10^{-3}	1.86×10^{-3}	6.32×14^{-3}
0.8	3.81×10^{-2}	4.14×10^{-3}	1.0×10^{-2}	1.90×10^{-3}	2.92×10^{-3}	2.83×10^{-3}
0.7	1.36×10^{-1}	1.41×10^{-2}	2.7×10^{-2}	8.78×10^{-3}	9.13×10^{-3}	8.81×10^{-3}
0.6	7.38×10^{-1}	6.32×10^{-2}	8.50×10^{-2}	1.77×10^{-2}	2.27×10^{-2}	2.20×10^{-2}
0.5	4.24	4.6×10^{-1}	7.46×10^{-1}	6.23×10^{-2}	5.47×10^{-2}	5.35×10^{-2}
0.4	1.75	8.83×10^{-1}	2.32	6.56×10^{-1}	4.68×10^{-1}	1.14×10^{-1}

The maximum relative error is the absolute value of the maximum difference between the true potential and imaging potential on the intermediate shell, divided by the maximum absolute value of the true potential on the intermediate shell, over the grid points used for plotting (Kearfott et al., 1991). Values in column 1 are from DCIT, and those in column 2 are from CCIT. The true data are produced by Eq. (A.2) in Appendix A for the known pair of dipoles, the imaging data ($r_I \le R$) of the DCIT are computed by Eq. (A.2), while the imaging data ($r_I \le R$) of the CCIT are computed by Eq. (A.1) in Appendix A. r_I is the radius of the imaging spherical shell, r_T is the radius of the test surface on which equivalent sources are placed.

3.2. Test 2: imaging a pair of point currents

Let us assume that a pair of point current sources are located at Cartesian coordinates $(x,y,z) = (\pm 0.3 \sin(\pi/6), 0.0, 0.3 \cos(\pi/6))$ and that their current strengths are ± 1.0 (keeping an overall neutrality of the source for the brain). The imaging errors of the CCIT and DCIT are shown in Table 2, and these errors suggest that the r_T for CCIT should be between 0.35 and 0.45, while for DCIT it had also better be smaller than 0.45. The results suggest that the CCIT is superior to the DCIT for imaging of current sources. The imaging maps, shown in Fig. 3, also suggest that CCIT is better than DCIT for the imaging of current sources. According to the theory in Amir (1994), the moment of the general equivalent dipole source is not necessarily normal to the surface and thus the radial equivalent dipole used in DCIT is not always an appropriate equivalent source for implementing CIT. However, the current sources/sinks are fundamental components of the arbitrary current dipoles, and proper current source/

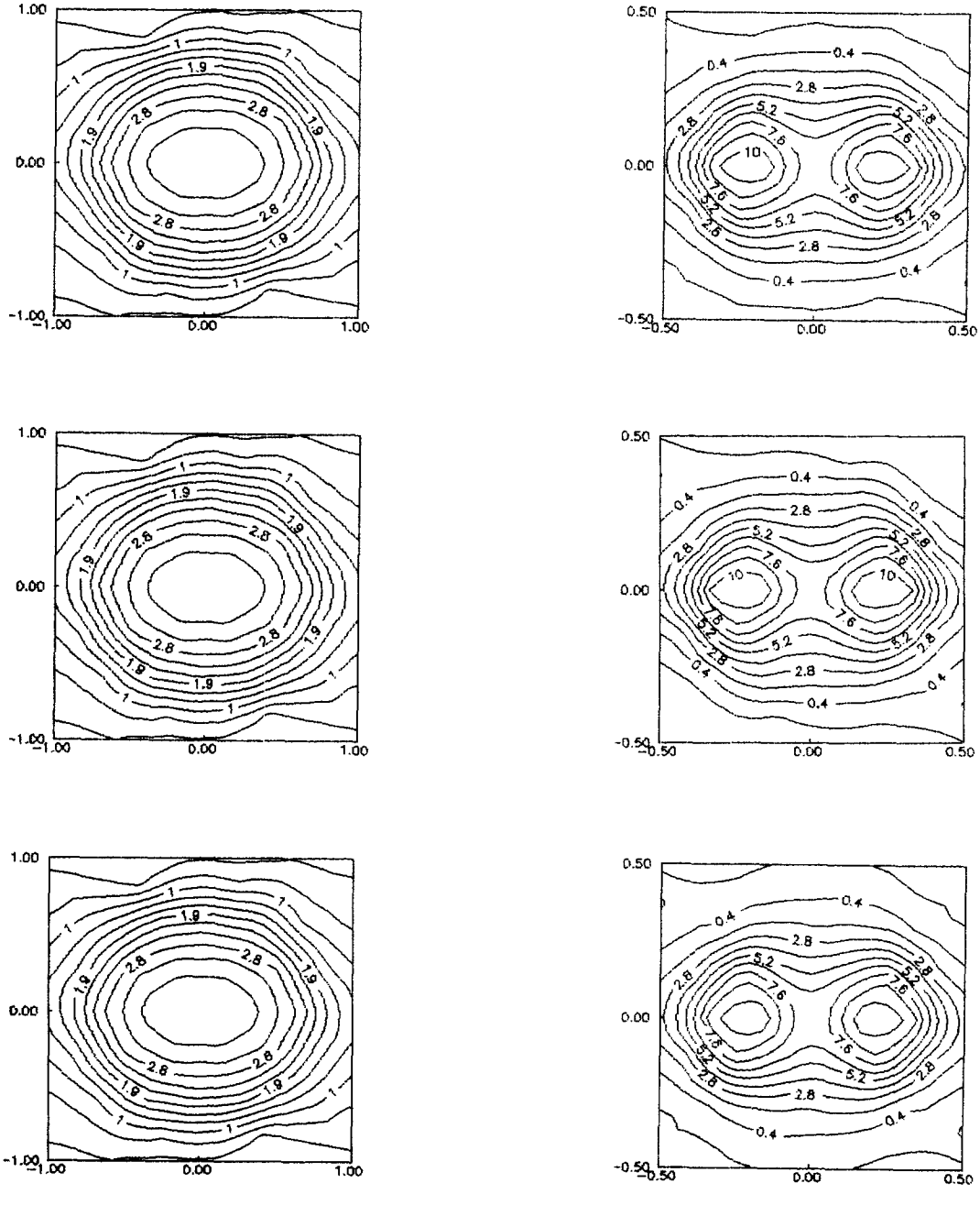

Fig. 2. The first row is the true data; the second row shows the imaging results produced by DCIT ($r_T = 0.35$); the third row shows the imaging maps produced by CCIT ($r_T = 0.35$). The imaging radius r_I is 1.0 (the surface of the 'head') for the left column and 0.5 for the right column.

Table 2
The maximum relative errors

r_I	r_T					
	0.55		0.45		0.35	
	(1)	(2)	(1)	(2)	(1)	(2)
1.0	6.03×10^{-3}	3.15×10^{-3}	5.27×10^{-3}	2.29×10^{-3}	3.29×10^{-3}	4.59×10^{-4}
0.8	1.04×10^{-1}	1.34×10^{-3}	2.23×10^{-2}	1.02×10^{-3}	4.29×10^{-3}	6.19×10^{-4}
0.7	3.67×10^{-1}	5.62×10^{-3}	7.94×10^{-2}	2.63×10^{-3}	1.68×10^{-2}	1.74×10^{-3}
0.6	1.81	4.11×10^{-2}	2.46×10^{-1}	6.29×10^{-3}	4.13×10^{-2}	3.76×10^{-3}
0.5	2.98	3.87×10^{-1}	1.16	4.64×10^{-2}	1.04×10^{-1}	1.14×10^{-2}
0.4	2.87	8.14×10^{-1}	3.50	5.34×10^{-1}	4.49×10^{-1}	5.32×10^{-2}

The meanings of the symbols used here are same as for Table 1, however, the true data here are computed by Eq. (A.1) for the known pair of point currents.

sink combinations may provide a valid explanation of both the potentials generated by current sources and those generated by dipoles. Thus, the CCIT may be used for both dipole and point current imaging problem, whereas the DCIT is more efficient for the radial dipole problem as that in test 1 above than for the point current problem such as that in test 2.

4. Conclusion and discussion

The point current source is suggested as a new kind of equivalent source in CIT. Numerical tests and comparison with the original CIT have been performed, and the results show that both equivalent dipole and equivalent point current are effective for imaging a pair of dipoles, while for imaging a pair of point current sources, the equivalent point current source is superior to the equivalent dipole source. However, both the original CIT (noted DCIT above) and the suggested CIT (noted CCIT above) still suffer form lack of proper theory which justifies the equivalent source techniques in the form of either equivalent radial dipoles or point sources. This poses an interesting problem for investigation in the future.

Appendix A

According to Frank (1952), the expression of the electric potential ψ_0 produced by a point current source in a homogenous conducting sphere is

$$\psi_0 = \frac{I}{4\pi\delta}\left(\frac{1}{r_q}+\frac{r_I}{R^2}+\frac{R}{r_{qi}}-\frac{1}{R}-\frac{1}{R}\ln\frac{r_{qi}+R^2-s}{2R^2}\right) \quad \text{(A.1)}$$

where I is the strength of current, R is the radius of the sphere. Let the point current source locate a $\boldsymbol{x}_q(x_{q1},x_{q2},x_{q3})$ and the field point ar $\boldsymbol{r}_I(x_{i1},x_{i2},x_{i3})$, then the other quantities in Eq. (A.1) may be defined as

$$r_q = \left(\sum_{k=1}^{3}(x_{ik}-x_{qk})^2\right)^{1/2}$$

$$r_I = (x_{i1}{}^2 + x_{i2}{}^2 + x_{i3}{}^2)^{1/2}$$

$$r_T = \left(\sum_{i=1}^{3}(x_{qi})^2\right)^{1/2}$$

$$r_{qi} = R^2\left(1+\frac{r_T^2 r_I^2}{R^4}-\frac{2s}{R^2}\right)^{1/2}$$

$$s = \sum_{k=1}^{3} x_{ik}x_{qk}$$

δ is the conductivity of the sphere. If a radial dipole with unit strength is located at point $\boldsymbol{x}_q$ on the surface of the test sphere with radius r_T, then the potential produced by the radial dipole at point r_I on the imaging spherical surface with radius r_I is (Kearfott et al., 1991)

$$V(\boldsymbol{x}_q,\boldsymbol{r}_I) = \frac{1}{4\pi\delta}\left[\frac{r_I\cos\theta - r_T}{(r_I^2+r_T^2-2r_T r_I\cos\theta)^{3/2}} + \frac{r_I\cos\theta - r_I^2 r_T}{(1+(r_I r_T)^2-2r_T r_I\cos\theta)^{3/2}} + \frac{1}{r_T(1+(r_I r_T)^2-2r_T r_I\cos\theta)^{1/2}} - \frac{1}{r_T}\right] \quad \text{(A.2)}$$

where θ is the angle between $\boldsymbol{r}_I$ and $\boldsymbol{x}_q$.

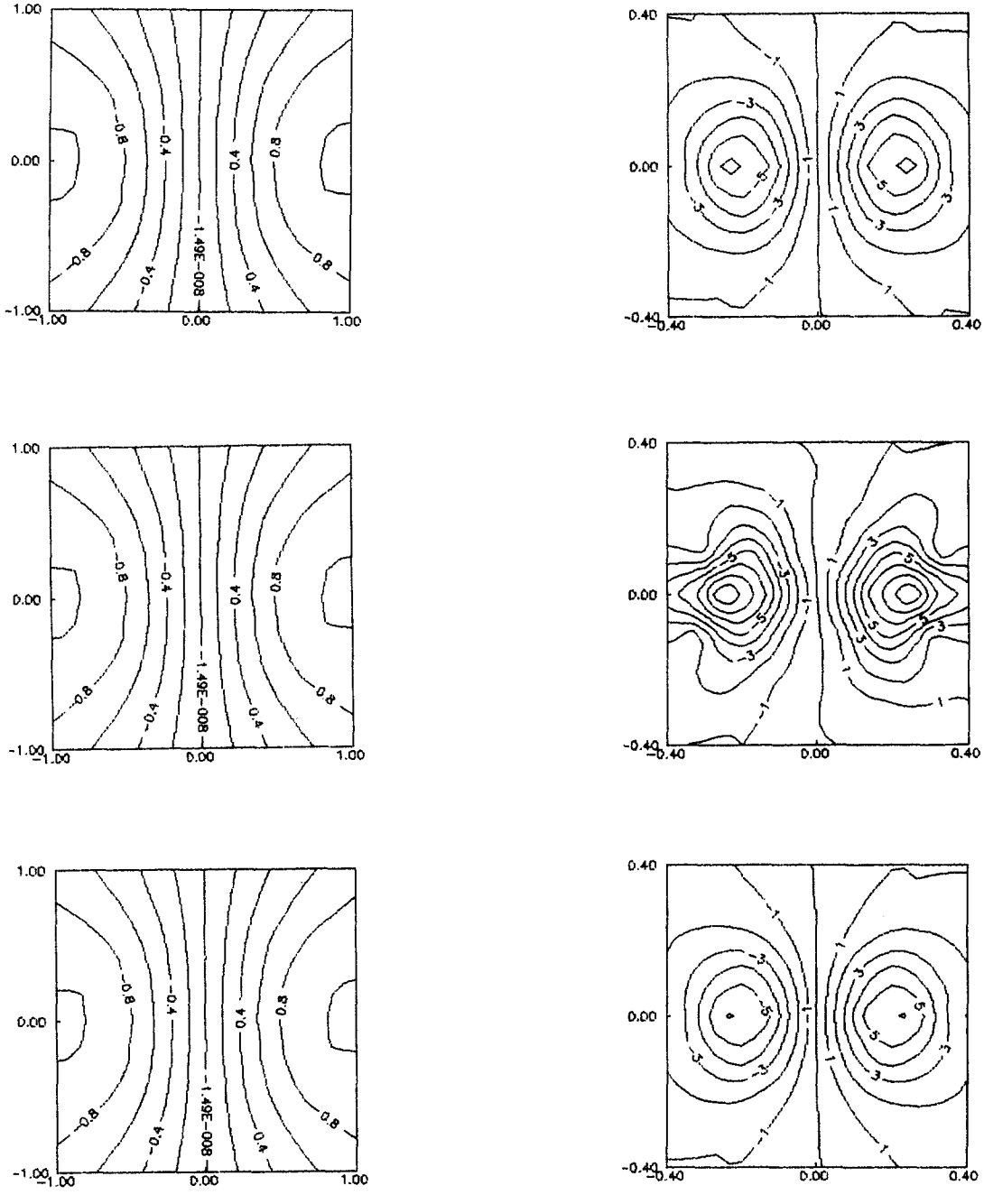

Fig. 3. The first row shows the true data; the second row shows the imaging results form DCIT ($r_T = 0.35$); and the third row shows the imaging maps from CCIT ($r_T = 0.35$). The imaging radius r_I is 1.0 for the left column and 0.4 for the right column.

Acknowledgements

We wish to thank Robert D. Sidman for informing us of the most useful references, we also thank F. Mauguière, L.G. Larrea and other unknown referees for their constructive comments on this paper.

References

Amir, A. Uniqueness of the generators of brain evoked potential maps. IEEE Trans. BME, 1994, 41: 1–11.

Dampney, C.N.G. The equivalent source technique. Geophysics, 1969, 34: 39–553.

Ford M.R., Sidman, R.D. and Ramsey, G. Spatio-temporal progression of the AEP P300 component using the cortical imaging technique. Brain Topogr., 1993, 6: 43–50.

Frank, E. Electric potential produced by two point current sources in a homogeneous conducting sphere. J. Appl. Phys., 1952, 23: 1225–1228.

Kearfott, R.B., Sidman, R.D., Major, D.J. and Hill, C.D. Numerical tests of a method for simulating electric potentials on the cortical surface. IEEE Trans. BME, 1991, 38: 294–299.

Sidman, R.D. A method for simulating intracerebral potential fields: the cortical imaging technique. J. Clin. Neurophysiol., 1991, 8: 432–441.

Sidman, R.D., Ford, M.R. Ramsey, G. and Schlichting, C. Age-related features of the resting and P300 auditory evoked responses using the dipole location method and cortical imaging technique. J. Neurosci. Methods, 1990, 33: 23–32.

Sidman R.D., Major D.J., Ford, M.R. Ramsey, G. and Schlichting, C. Age-related features of the resting pattern-reversal visual evoked response using the dipole location method and cortical imaging technique. J. Neurosci. Methods, 1991, 37: 27–36.

Sidman, R.D., Vincent, D.J., Smith, D.B. and Lu Lee. Experimental tests of the cortical imaging technique-applications to the response to the median nerve stimulation and the location of epileptiform discharges. IEEE Trans. Biomed. Eng., 1992, 39: 437–444.

Wang, Y. and Yang, F. Three dimensional mapping of EEG. Chinese J. Med. Instrum., 1993, 17: 187–194 (in Chinese).